Electronic Supplementary Information (ESI)

For

Stomatocyte-like hollow polydopamine nanoparticles for rapid removal of water-soluble dyes from water

Jiayou Lin,[a] Haibo Wang, [a] Erhui Ren,[a] Qingshuan Song,[a] Jianwu Lan,[a] Sheng Chen,[a] * Bin Yan [ab] *

[a] *College of Biomass Science and Engineering, Sichuan University, Chengdu, 610065, China*
[b] *National Engineering Laboratory for Clean Technology of Leather Manufacture, Sichuan University, Chengdu, 610065, China*

E-mail addresses:
chensheng@scu.edu.cn (S.C.)
yanbinscu@126.com (B.Y.)

Materials

Dopamine hydrochloride (DA) and tetraethylorthosilicate (TEOS) (99 %) were purchased from Sigma Aldrich. Ammonium (25 %), ethanol, hydrofluoric acid (HF) (40 %), methylene blue (MB), methyl violet (MV), malachite green oxalate (MGO), Rhodamine B (RHB), hydrochloric (HCl) and sodium hydroxide (NaOH) were purchased from Chemical Co. Ltd, Chengdu, China. All chemicals were analytical grade and used without further purification. The aqueous solutions of different dyes were prepared with Deionized water (18.2 MΩ).

Characterizations

The morphology of samples was studied by a Transmission Electron Microscopy (TEM, Tecnai G2 F20 S-TWIN, FEI) operated at 200 kV and a field-emission Scanning Electron Microscopy (FE-SEM, JSM-5900LV, JEOL) operated at 15 kV. Fourier-transform infrared (FTIR) spectra were recorded on a Nicolet Avatar 370 spectrometer. The spectra were recorded over a frequency ranging from 400-4000 cm^{-1} with a spectral resolution of 2 cm^{-1}. The specific surface areas of the as-prepared adsorbents were measured on a Micromeritics Gemini VII 3.04 nitrogen-adsorption

apparatus (Micromeritics Instrument Corporation, America) using the Brunauer−Emmett−Teller (BET) method at a relative pressure ratio ranging from 0 to 1 at 77 K. The specific surface area and pore size distribution were calculated from a multipoint analysis of the volume of nitrogen adsorbed as a function of relative pressure. Ultraviolet-visible (UV-vis) spectra were recorded via a TU-1900 UV-vis spectrometer (Beijing Purkinje General Instrument Co. Ltd) at room temperature over the range of 400~800 nm. The pH of the solution was measured through a pH meter (Mettler Toledo Co., Ltd., Shanghai, China). Zeta potential measurements were performed on Nano ZSP (ZEN5600, Malvern instruments Co. Ltd).

Synthesis of stomatocyte-like hollow PDA nanoparticles (SHPNs). Briefly, 0.5 mL of ammonium was mixed with 12 mL of ethanol and 40 mL of deionized water. After stirring for 1 h, 0.5 mL of TEOS was added dropwise into the above mixture with another 30 min stirring. After that, 0.2 g of DA was added and the resulting mixture was stirred for 24 h. To promote further PDA polymerization, the obtained black suspension was hydrothermally treated in an autoclave at 413 K for another 24 h. The resultant black precipitate was collected by centrifuge at 8000 rpm for 10 min, followed by washing with ethanol and deionized water for several times until the supernatant was transparent. Finally, SHPNs were obtained by mixing the above product with HF solution (40 wt%) at 298 K for 2 h, followed by washing with abundant deionized water until the supernatant became neutral. The obtained SHPNs were collected by centrifuge and redispered in deionized water for further use.

Thermodynamic studies of adsorption. The adsorption experiments were carried out at 298 K. 0.5 mg of SHPNs were added into 10 mL of MB solution of different initial concentration ranging from 50 to 400 mg/L and the resulting suspensions were stirred for 30 min to approach equilibrium. The supernatant was separated by centrifuge at 8000 rpm for 10 min and analyzed by UV-vis spectroscopy.

Two adsorption isotherm models, including Langmuir (1) and Freundlich (2), were generated by plotting q_e versus C_e using the following equations：

$$q_e = \frac{q_{max} K_L C_e}{1 + K_L C_e} \quad (1)$$

$$q_e = K_F C_e^{\frac{1}{n}} \quad (2)$$

where q_e (mg g^{-1}) is the amount of MB adsorbed at equilibrium, q_{max} (mg g^{-1}) is the theoretical maximum adsorption capacity of SHPNs at equilibrium, C_e(mg L^{-1}) is the residual MB concentration at equilibrium, K_L is (mol^{-1}) is Langmuir equilibrium constant. K_F is Freundlich equilibrium constant, n is a coefficient to judge difficulty of adsorption possess.

Thermodynamic studies of SHPNs to other water-soluble cationic dyes, including Eschenmoser-containing dyes like MV and MGO as well as cationic RHB without Eschenmoser structure, were also performed using the same protocol as MB.

pH effect on the adsorption of SHPN to MB. 0.5 mg of SHPNs were mixed with a series of MB solutions (100 mg/L, 10 mL) with different pH ranging from 1 to 10. After stirring at 298 K for 30 min to reach adsorption equilibrium, the supernatant was separated by centrifuge at 8000 rpm for 10 min and analyzed by UV-vis spectroscopy.

Batch adsorption kinetics studies. The experiments were performed in 20 mL vials equipped with magnetic stir bars at 298 K. In a typical adsorption kinetics studies, 20 ml of MB (50 mg/L) was mixed up with 1 mg of SHPNs in the vials. The mixture was immediately stirred and 2 mL of the solution was taken at scheduled intervals via a syringe and filtered immediately by 0.22 μm PVDF membrane filter. The residual concentration of MB in each sample was determined by UV-vis spectroscopy.

MB removal efficiency (in %) by SHPNs was determined by the following equation：

$$\text{MB removal efficiency} = \frac{C_0 - C_t}{C_0} \times 100 \quad (3)$$

where C_0 (mg L^{-1}) and C_t (mg L^{-1}) are the initial and residual concentration (at

different time) of MB. The following equation was used to determine the amount of MB adsorbed by SHPNs：

$$q_t = \frac{(C_0 - C_t)V}{m} \quad (4)$$

where q_t (mg g^{-1}) is amount of MB adsorbed by SHPNs at time *t* (min). C_0 (mg L^{-1}) and C_t (mg L^{-1}) are the initial and residual concentration of MB. *m* (g) is the mass of SHPNs used in the study. *V* (L) is the volume of the mixture of MB solution and SHPNs.

The MB uptake rate of SHPNs was fitted by pseudo-first-order and pseudo-second-order adsorption models, which are expressed as the following equations in a general linearized form：

$$ln\ (q_e - q_t) = ln\ q_e - k_1 t \quad (5)$$

$$\frac{t}{q_t} = \frac{t}{q_e} + \frac{1}{k_2 q_e^2} \quad (6)$$

where q_t and q_e are the adsorbate uptake (mg g^{-1}) at time *t* (min) and at equilibrium，respectively, and k_1 is first-order rate constant (min^{-1}) and k_2 is second-order rate constant (g mg^{-1} min^{-1}).

As a control experiment, solid polydopamine microsphere (SPM)[1] was also synthesized according to a reported procedure and the same protocol as SPHNs was applied to determine its adsorption kinetics to MB.

The flow-through experiments on SHPNs and SPM. 0.5 mg of SHPNs were separately immobilized on 0.2 μm PVDF syringe filters as a thin layer, and aqueous MB solution (4 ml, 50—90 mg/L) was passed quickly through the filter at a flow rate of 0.1 mL/s under room temperature. The filtrate was analyzed by UV-vis spectroscopy. For comparison, the flow-through experiment on SPM was also tested using the same procedure.

SHPNs recycling experiments. 0.5 mg of SHPNs were added into 10 mL of MB solution (100 mg/L). The mixture was stirred at 298 K for 30 min, and then filtered to collect the filtrate for UV-vis measurement. The collected SHPNs were reborn by

washing with acidic ethanol solution (0.1 M HCl) for several times until the filtrate was colorless. The regenerated SHPNs were reused in the adsorption experiment. The whole above recycling process was repeated 13 times to determine its practice application.

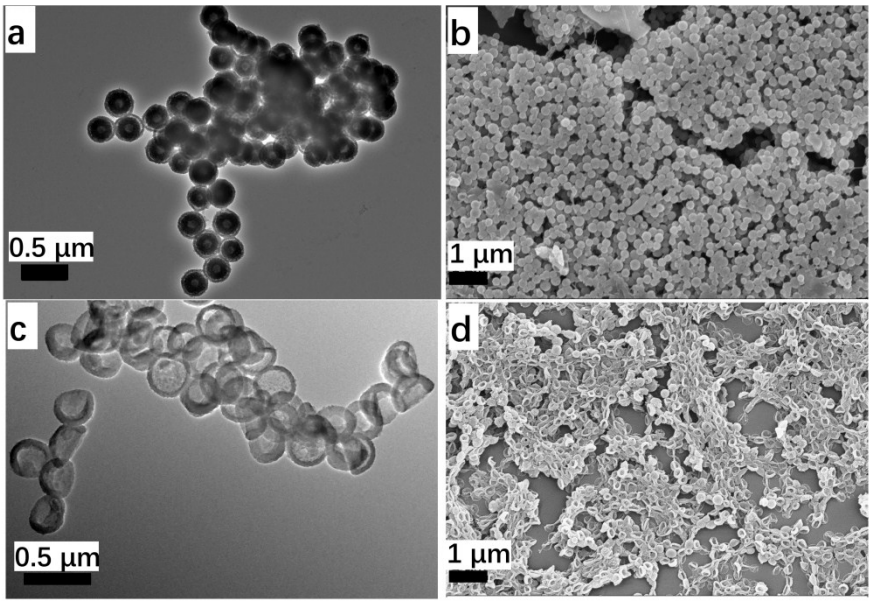

Fig. S1 Microscopy characterizations of the SiO_2@PDA nanoparticles and SHPN: a) TEM and b) SEM images show the core-shell structure of the SiO_2@PDA nanoparticles after hydrothermal treatment at 140 °C for 24 h; c) TEM and d) SEM images show the stomatocyte-like hollow morphology of SHPN prepared from the SiO_2@PDA nanoparticles after HF etching for 2 h.

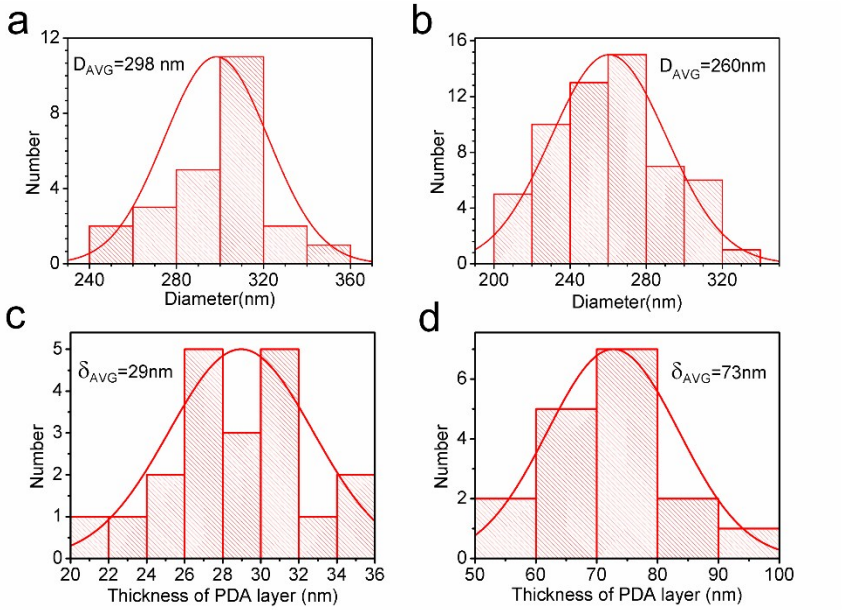

Fig. S2 The diameter of (a) the SiO_2@PDA nanoparticles after hydrothermal treatment and (b) SHPNs as well as the thickness of PDA layers on (c) the corresponding SiO_2@ PDA nanoparticles (d) SHPNs.

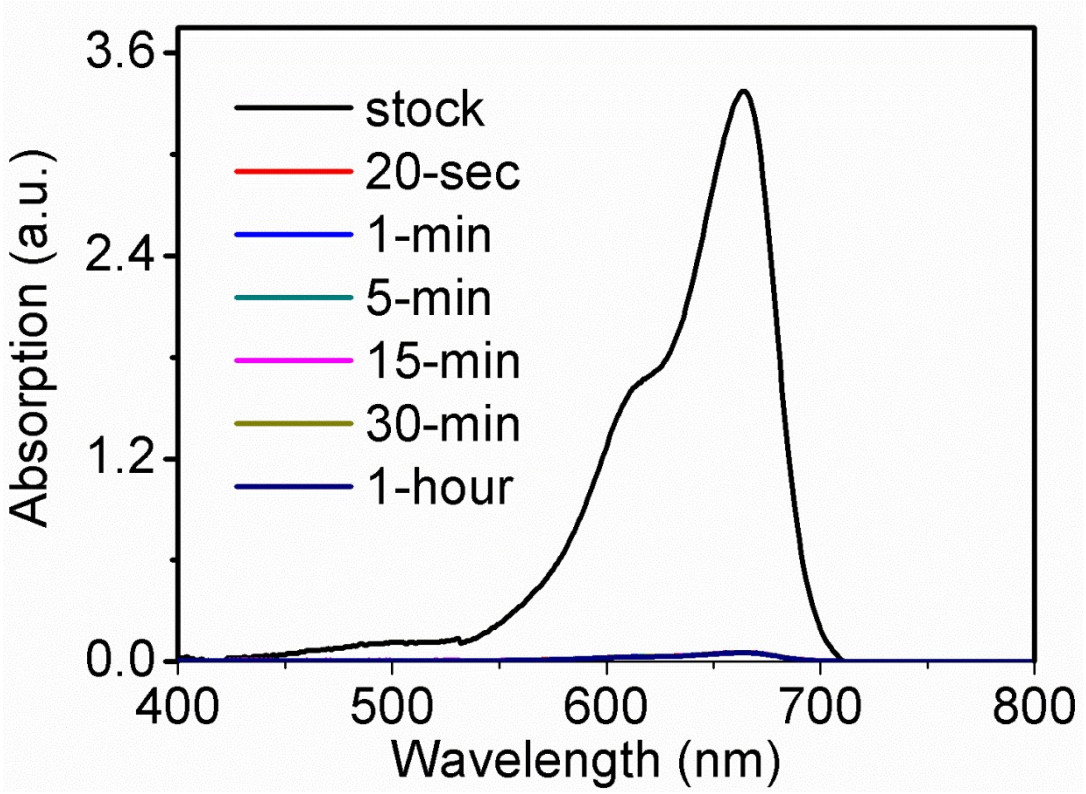

Fig. S3 Characterization of MB uptake kinetics by SHPNs. UV-vis spectra of the supernatant recorded at different contact time after mixing SHPNs with MB solution.

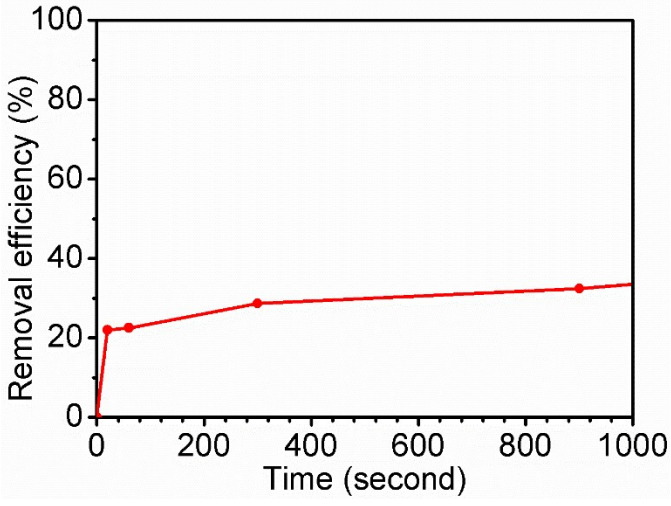

Fig. S4 MB adsorption kinetics of SPM with MB concentration of 50 mg/L.

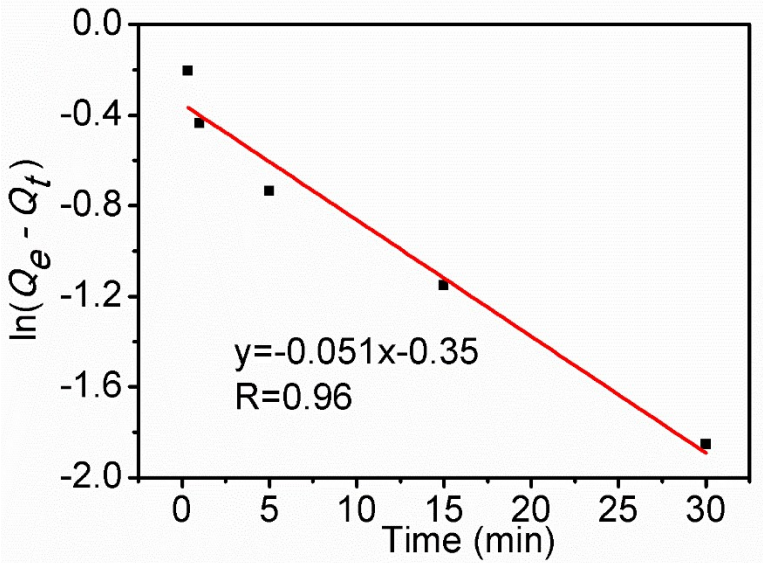

Fig. S5 The data of adsorption kinetics experiments was fitted with pseudo-first-order model. The adsorption kinetic behaviors of SHPNs are not well described by the pseudo-first-order model with a correlation of 0.96.

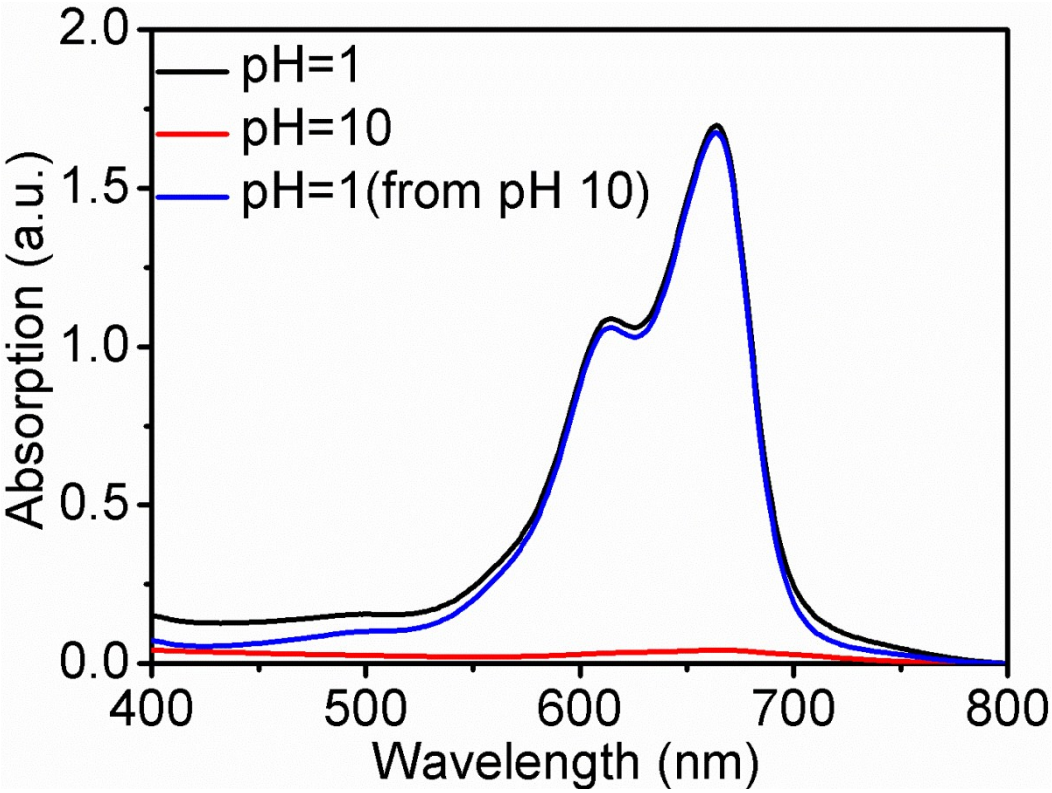

Fig. S6 Effect of pH on the adsorption of SHPNs to MB. SHPNs were mixed with MB solutions with different pH values (pH =1 and 10). After reaching adsorption equilibrium, the supernatant

was centrifuged out and analyzed by UV-vis. The inset shows images of the supernatants separated by centrifuge after adsorption at different pH values.

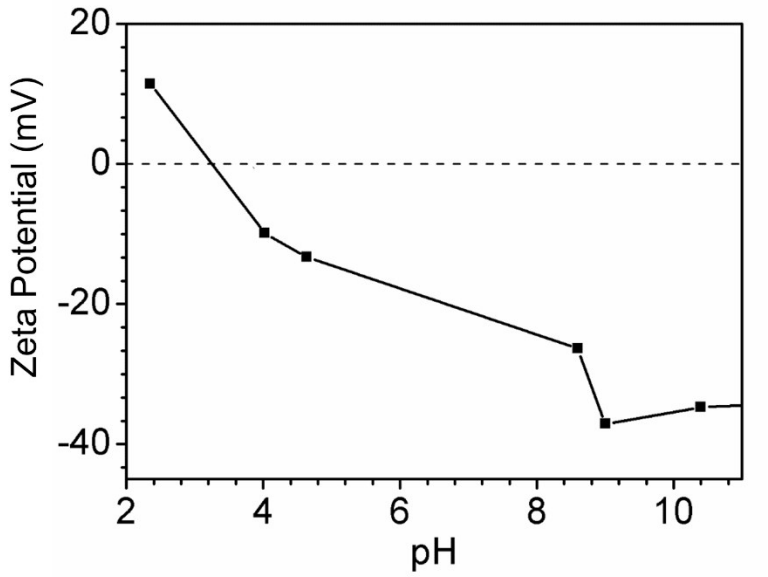

Fig. S7 Zeta potential of SHPNs as a function of pH of the solution.

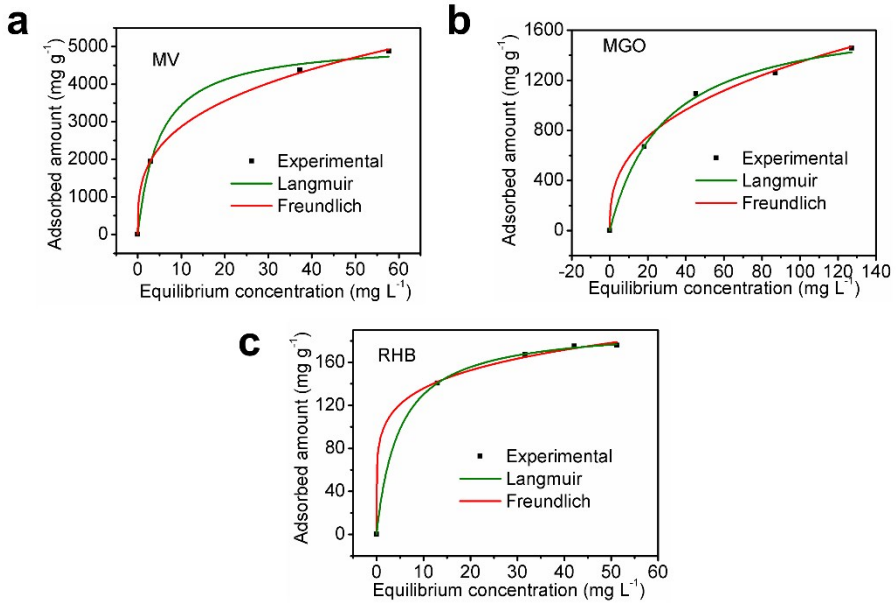

Fig. S8 The adsorption isotherm for SHPN to different water-soluble dyes (a) MV, (b) MGO, and (c) RHB at different initial concentration (including 0.5 mg of SHPNs and 10 ml dye solution) and the data was fitted with nonlinear isotherm models, such as Langmuir and Freundlich.

Table S1 Adsorption capacity and adsorption rate of MB on different PDA-based adsorbents

PDA-based adsorbent	*Qe* (mg g^{-1})	K_2 (g mg^{-1} min^{-1})
PDA@Fe_3O_4@PEI[2]	172.4	$3.4*10^{-3}$
PVDF/PDA[3]	172.3	-----
MPDA[4]	150	-----
Fe_3O_4/PDA[5]	204.1	-----
MF@Fe_3O_4@PDA/PSBMA[6]	344	$4.9*10^{-3}$
BAC-PDA[7]	182	-----
PDA-rGO-kaolin[8]	39.6	$1.7*10^{-3}$
PIL@PDA@Fe_3O_4[9]	72.5	
PDA microspheres[1]	88.89	$1*10^{-3}$
PDA-67 aerogel[10]	153.4	$3.3*10^{-5}$
MSM-PDA[11]	83.8	$1.18*10^{-3}$
SAB-PDA[12]	2276	$1.68*10^{-3}$
GO-PDA[13]	1800	-----
This work	3200	0.43

Table S2 The Parameters related to pseudo-second-order adsorption kinetics models of SHPN and SPM

Adsorbents	Parameters	Value	R^2
SHPN	q_e (mg g^{-1})	980	0.99
	K_2(g $mg^{-1}min^{-1}$)	4.3×10^{-1}	
SPM	q_e (mg g^{-1})	546	0.96
	K_2 (g mg^{-1} min^{-1})	4.3×10^{-4}	

Table S3 Parameters of nonlinear Langmuir and Freundlich model for adsorption of MB, MV, MGO, and RHB.

	Nonlinear Langmuir model		
	q_{max} (mg g^{-1})	K_L (L mg^{-1})	R^2
MB	2896	0.550	0.9736
MV	5137	0.202	0.9965
MGO	1748	0.035	0.9953
RHB	194	0.204	0.9998
	Nonlinear Freundlich model		
	K_F ((L/mg)$^{1/n}$)	1/n	R^2
MB	1372	0.152	0.9673
MV	1409	0.309	0.9991
MGO	252	0.363	0.9921
RHB	92	0.169	0.9988

References:

1 J. Fu, Z. Chen, M. Wang, S. Liu, J. Zhang, J. Zhang, R. Han and Q. Xu, *Chem. Eng. J.*, 2015, **259**, 53.

2 Z. Wang, J. Guo, J. Ma and L. Shao, *J. Mater. Chem. A*, 2015, **3**, 19960.

3 F. F. Ma, N. Zhang, X. Wei, J. H. Yang, Y. Wang and Z. W. Zhou, *J. Mater. Chem. A*, 2017, **5**, 14430.

4 F. Chen, Y. Xing, Z. Wang, X. Zheng, J. Zhang and K. Cai, *Langmuir*, 2016, **32**, 12119.

5 S. Zhang, Y. Zhang, G. Bi, J. Liu, Z. Wang, Q. Xu, H. Xu and X. Li, *J Hazard Mater*, 2014, **270**, 27.

6 Y. Q. Zhang, X. B. Yang, Z. X. Wang, J. Long and L. Shao, *J. Mater. Chem. A*, 2017, **5**, 7316.

7 E. I. El-Shafey, S. N. F. Ali, S. Al-Busafi and H. A. J. Al-Lawati, *J. Environ. Chem. Eng.*2016, **4**, 2713.

8 K. He, G. Zeng, A. Chen, Z. Huang, M. Peng, T. Huang and G. Chen, *Compos. Part B-Eng.*, 2019, **161**, 141.

9 Y. Lu, H. Zhu, W.-J. Wang, B.-G. Li and S. Zhu, *ACS Sustain. Chem. Eng.*, 2017, **5**, 2829.

10 X. Wei, T. Huang, J. Nie, J. H. Yang, X. D. Qi, Z. W. Zhou and Y. Wang, *Carbohydr. Polym.*, 2018, **198**, 546.

11 T. Ataei-Germi and A. Nematollahzadeh, *J. Colloid Interface Sci.*, 2016, **470**, 172.

12 N. Mahmoodi-Babolan, A. Nematollahzadeh, A. Heydari and A. Merikhy, *Int. J. Biol. Macromol.*, 2018, **125**, 690.

13 Z. Dong, D. Wang, X. Liu, X. Pei, L. Chen and J. Jin, *J. Mater. Chem. A*, 2014, **2**, 5034.